

000
001
002
003

SPARSE FEATURE ROUTING FOR TABULAR LEARNING

004
005
006
007
008009 **Anonymous authors**
010
011
012
013
014
015
016
017
018
019
020
021
022
023
024
025
026
027028 Paper under double-blind review
029
030
031
032
033
034
035
036
037
038
039
040
041
042
043
044
045
046
047
048
049
050
051
052
053

ABSTRACT

The landscape of high-performance tabular learning is often framed as a choice between the efficiency of gradient-boosted trees and the performance of deep architectures, which increasingly rely on heavy, monolithic backbones to model feature interactions. We argue that this monolithic design overlooks a critical inductive bias: the inherent sparsity and modularity of tabular data. To address this, we introduce the Sparse Feature Routing Network (SFR Net), an architecture that decomposes computation into independent feature experts controlled by an entropy-regularized router, coupled with a low-rank module to capture non-additive dependencies. We evaluate SFR Net across 14 heterogeneous benchmarks, including standard datasets, high-dimensional multiclass tasks, and regression problems. Empirically, SFR Net demonstrates predictive performance competitive with, and often superior to, state-of-the-art deep tabular models and gradient-boosted ensembles. Beyond raw performance, SFR Net offers three distinct structural advantages: (1) efficiency, requiring up to $24\times$ fewer parameters and training $30\times$ faster than tabular Transformers; (2) intrinsic sparsity, dynamically activating only a small fraction of features per instance; and (3) faithful interpretability, where deletion tests confirm that the learned routing weights serve as reliable, causal instance-level attributions. These results position sparse feature routing as a lightweight, transparent, and high-performance alternative to dense tabular foundation models.

1 INTRODUCTION

Tabular data are among the most widespread data modalities, arising in domains such as healthcare, finance, and the social sciences. Despite their ubiquity, learning effective representations from tabular datasets remains a fundamental challenge. Unlike image, text, or audio inputs, tabular records consist of heterogeneous features of varying types and scales, often with weak or irregular dependencies. These characteristics limit the transfer of inductive biases that have powered deep learning breakthroughs in unstructured modalities. As a result, classical approaches such as gradient-boosted decision trees remain dominant in practice, while neural networks have historically struggled to consistently outperform them.

Recent research has begun to narrow this gap by improving training strategies, designing novel architectures, and exploring self-supervised objectives tailored to tabular domains. Advances in normalization, regularization, and feature encoding have enhanced the robustness of deep models, while architectural innovations such as attention mechanisms and modular processing blocks have sought to capture complex feature interactions. In parallel, representation learning methods have shown that self-supervision can extract informative embeddings without labels, improving downstream classification and regression tasks. Yet, despite this progress, a core difficulty persists: most existing models still treat tabular inputs monolithically, processing all features through shared encoders. This design blurs the role of individual columns, complicates interpretability, and can reduce robustness in the presence of irrelevant or noisy features.

In this work, we propose the **Sparse Feature Routing Network (SFR Net)**, a new architecture designed to address these limitations. Our approach decomposes each feature into a specialized expert network, ensuring that heterogeneous columns are modeled according to their individual distributions. These experts are then dynamically composed by a lightweight router that assigns sparse, entropy-regularized attention weights, selecting only the most informative features for each instance. This design provides three key advantages: (i) principled handling of heterogeneity through feature-

wise specialization, (ii) efficiency and robustness via sparse routing that scales with feature count and resists irrelevant inputs, and (iii) native interpretability, as the router’s weights yield direct, transparent per-instance attributions without the need for post-hoc analysis.

Beyond raw performance, the novelty of SFR Net lies in introducing sparse, feature-level routing as an inductive principle for tabular learning. While previous approaches have relied on either dense transformations of all features or indirect mechanisms such as mask prediction, our framework directly encodes the idea that each column should contribute selectively and independently to the decision process. This perspective not only improves predictive accuracy but also aligns with how practitioners naturally interpret tabular data—by analyzing the marginal and conditional relevance of individual features. In doing so, SFR Net provides a step toward architectures that are not only competitive with established baselines but also inherently interpretable and resilient under distributional shifts.

Our contributions can be summarized as follows:

- **Feature-wise specialization with sparse routing.** We introduce a feature-expert decomposition with an entropy-regularized router that performs instance-conditioned, sparse selection, providing a principled inductive bias for heterogeneous tabular data.
- **Competitive accuracy without pre-training.** SFR Net achieves performance competitive with or superior to recent deep learning methods across a range of tabular benchmarks, while avoiding complex self-supervised pre-training and maintaining a simple, efficient architecture.
- **Native interpretability and efficiency.** The router’s sparse weights yield direct, explicit per-instance attributions from the model itself, removing the need for post-hoc methods. The architecture scales linearly with feature count, allowing effective training even on CPUs.

2 RELATED WORK

2.1 SPARSE FEATURE-EXPERT ROUTING

Conditional computation has long been studied as a way to scale neural models while improving efficiency and interpretability. The Mixture-of-Experts (MoE) paradigm (Jacobs et al., 1991; Shazeer et al., 2017; Lepikhin et al., 2021) routes inputs to one of several interchangeably-parameterized sub-networks, while developments in differentiable gating, such as `sparsemax` and `entmax` (Martins & Astudillo, 2016; Peters et al., 2019), provide tools to enforce controllable top- k sparsity. Our work adopts these ideas but reframes the target of sparsity. Instead of routing between global experts that all see the entire input, we introduce *feature-expert routing*, where each input feature is assigned its own dedicated expert network and sparsity is applied directly at the feature level.

Low-rank interaction modules such as factorization machines (Rendle, 2010), cross networks (Wang et al., 2021), and high-order interaction blocks play a complementary role by capturing higher-order dependencies efficiently. In most prior work, however, these interactions are embedded in monolithic backbones, making it difficult to relate them back to individual features. SFR Net departs from this tradition by combining instance-wise sparse routing over feature-specific experts with a rank-controlled mixer, explicitly tying interaction capacity to a small number of low-rank factors.

2.2 TABULAR DEEP LEARNING AND FOUNDATIONAL MODELS

A large body of work has explored deep architectures for supervised learning on tabular data, including attention-based models (e.g., TabTransformer, FT-Transformer) (Huang et al., 2020; Gorishniy et al., 2021), retrieval-augmented models (Somepalli et al., 2021; Gorishniy et al., 2024; Ye et al., 2024), and capsule-like or compositional architectures (Chen et al., 2023). Generalized additive models and Neural Additive Models (NAMs) (Agarwal et al., 2021) emphasize per-feature structure and interpretability by enforcing a global additive decomposition, but do not support sample-specific expert selection or controlled non-additive interactions.

More recently, *tabular foundation models* have emerged, aiming for broad coverage across diverse datasets. TabPFN and its successors (Hollmann et al., 2023) use transformers trained in a meta-

108 learning fashion to amortize inference over synthetic tasks, while RealMLP, TabDPT, TabICL, and
 109 LimiX refine MLP-based designs with better regularization, pre-training objectives, or in-context
 110 learning strategies. TabM (Gorishniy et al., 2025) provides an especially strong and practical MLP-
 111 based baseline: by combining parameter-efficient BatchEnsemble-style ensembling with per-feature
 112 embeddings and careful tuning on a 46-dataset benchmark, TabM achieves the best average rank
 113 among deep tabular models and competes with GBDTs in both performance and efficiency. These
 114 results show that well-engineered MLPs are stronger than many attention- and retrieval-based archi-
 115 tectures, and they frame simple MLPs and TabM as robust default baselines.

116 Our work is complementary to this line. Foundational tabular models typically operate on dense,
 117 shared feature representations and do not implement instance-wise sparse routing over feature-
 118 specific experts. SFR Net instead treats sparsity and feature-wise modularity as the central archi-
 119 tectural principle. On OpenML-CC18, we compare against the state-of-the-art landscape and report
 120 that SFR Net is competitive with strong deep baselines.

121

122 2.3 REPRESENTATION LEARNING FOR TABULAR DATA

123

124 Self-supervised learning (SSL) has been successfully adapted to tabular domains through objectives
 125 such as masked feature reconstruction, contrastive learning, and sub-sampling tasks (Yoon et al.,
 126 2020; Bahri et al., 2022; Ucar et al., 2021). These approaches typically pre-train a monolithic en-
 127 coder and then fine-tune it for downstream supervised tasks, often using transformers or ResNet-like
 128 backbones. Recent work on tabular JEPA-style models further explores predictive objectives that op-
 129 erate on structured partitions of the input. While powerful, such methods often require substantial
 130 pre-training compute and do not expose feature-wise structure directly.

131 SFR Net instead relies on a single supervised training phase and encodes inductive biases directly
 132 in the architecture: feature-wise experts, sparse instance-wise routing, and a low-rank interaction
 133 head. Our experiments compare SFR Net against SSL-enhanced ResNet models on our core bench-
 134 marks and show that explicit feature-level structure can match or surpass SSL backbones on several
 135 datasets, despite the absence of pre-training.

136

137 **Relation to Neural Additive Models.** Neural Additive Models (NAMs) enforce a globally additive
 138 decomposition of the form $f(x) = \sum_j f_j(x_j)$, which yields strong interpretability at the cost
 139 of limited interaction capacity. SFR Net differs in two fundamental ways. First, its router intro-
 140 duces *instance-wise sparsity*: for each sample, only a subset of feature experts is activated, whereas
 141 NAMs do not support sample-specific expert selection. Second, the low-rank interaction head in-
 142 troduces controlled non-additive interactions among the routed features, breaking strict additivity
 143 while keeping interaction capacity bounded. Our ablations and deletion tests empirically validate
 144 that these design choices yield both improved performance and faithful attributions.

145

146 3 METHOD

147

148 Our proposed **Sparse Feature Routing Network (SFR Net)** is designed to model tabular data by
 149 directly addressing the core challenge of feature heterogeneity through a modular and interpretable
 150 architecture, as illustrated in Figure 1. The model comprises three principal components: (1) a set
 151 of specialized **expert networks**, one for each input feature; (2) an instance-wise **sparse feature**
 152 **router** that dynamically selects the most relevant experts; and (3) a **low-rank interaction head** that
 153 efficiently captures higher-order dependencies among the selected features before making a final
 154 prediction.

155

156 3.1 FEATURE-WISE EXPERT NETWORKS

157

158 To effectively handle the diverse types and distributions inherent in tabular data, SFR Net eschews
 159 a monolithic encoder. Instead, for an input instance with F features, $\mathbf{x} = [x_1, x_2, \dots, x_F]$, each
 160 feature x_j is processed by its own dedicated expert network E_j . This “one-expert-per-feature”
 161 principle allows the model to learn specialized transformations tailored to the semantics of each
 162 column, producing a high-dimensional feature representation $\mathbf{h}_j \in \mathbb{R}^D$.

162 **Numeric Experts** For a scalar numerical feature x_j , the corresponding expert E_j^{num} is a small
 163 Multi-Layer Perceptron (MLP) that maps the scalar input to the D -dimensional representation space:
 164 $\mathbf{h}_j = \text{MLP}_{\text{num}}(x_j)$.
 165

166 **Categorical Experts** For a categorical feature x_j with cardinality C_j , the expert E_j^{cat} first projects
 167 it into a dense embedding space using an embedding layer Emb_j to obtain a vector $\mathbf{e}_j \in \mathbb{R}^{D_{\text{emb}}}$,
 168 which is then transformed by an MLP:

$$169 \quad \mathbf{h}_j = \text{MLP}_{\text{cat}}(\text{Emb}_j(x_j)).$$

170 For robustness to out-of-distribution data, the embedding layer for each categorical expert reserves
 171 a dedicated index to represent unknown categories encountered during inference.
 172

173 After processing all F features, we obtain a set of expert representations $\{\mathbf{h}_1, \dots, \mathbf{h}_F\}$, which are
 174 then conceptually stacked to form a representation matrix $\mathbf{H} \in \mathbb{R}^{F \times D}$ for the input instance.
 175

176 3.2 INSTANCE-WISE SPARSE FEATURE ROUTER

177 Rather than naively combining all feature representations, SFR Net employs a lightweight routing
 178 mechanism to perform instance-specific feature selection. The router learns to assign an attention
 179 weight α_j to each expert representation \mathbf{h}_j , effectively determining the importance of each feature
 180 for a given input.
 181

182 A shared scoring network—a simple MLP with a Tanh activation—computes a scalar score s_j for
 183 each feature representation. These scores are subsequently normalized into a probability distribution
 184 $\boldsymbol{\alpha} = [\alpha_1, \dots, \alpha_F]$ over the features using the softmax function:

$$185 \quad \alpha_j = \frac{\exp(s_j)}{\sum_{k=1}^F \exp(s_k)}. \quad (1)$$

186 To encourage the model to select a small subset of highly informative features, thereby inducing
 187 sparsity and improving interpretability, we introduce an entropy regularization term into the training
 188 objective. Minimizing the entropy of the attention distribution,
 189

$$190 \quad H(\boldsymbol{\alpha}) = - \sum_{j=1}^F \alpha_j \log(\alpha_j),$$

191 encourages $\boldsymbol{\alpha}$ to become “peaky,” concentrating its mass on a few features. In practice, we observe
 192 that reasonable values of the sparsity coefficient lead to 8–15% of features being effectively active
 193 per instance on our benchmarks, while preserving predictive performance.
 194

195 3.3 LOW-RANK INTERACTION AND PREDICTION HEAD

196 The sparse weights $\boldsymbol{\alpha}$ gate two parallel pathways. While the first captures additive effects, the second
 197 is designed to explicitly model higher-order relationships efficiently through a **low-rank interaction**
 198 **module**.
 199

200 **First-Order Representation** The first-order representation $\mathbf{r}^{(1)} \in \mathbb{R}^D$ is computed as the
 201 attention-weighted sum of the expert outputs, capturing the additive effects of the selected features:
 202

$$203 \quad \mathbf{r}^{(1)} = \sum_{j=1}^F \alpha_j \mathbf{h}_j. \quad (2)$$

204 **Higher-Order Interaction** Each expert representation \mathbf{h}_j is projected into two separate low-
 205 dimensional “key” and “value” spaces using shared projection matrices $\mathbf{W}_K, \mathbf{W}_V \in \mathbb{R}^{D \times K}$, where
 206 $K \ll D$ is the interaction rank. The interaction representation $\mathbf{r}^{(2)} \in \mathbb{R}^K$ is then computed as the
 207 element-wise product of the attention-weighted keys and values:
 208

$$209 \quad \mathbf{r}^{(2)} = \sum_{j=1}^F \alpha_j (\mathbf{k}_j \odot \mathbf{v}_j), \quad \text{where } \mathbf{k}_j = \mathbf{h}_j^\top \mathbf{W}_K, \mathbf{v}_j = \mathbf{h}_j^\top \mathbf{W}_V. \quad (3)$$

This formulation efficiently captures second-order interactions between the routed features under an explicit rank budget K . The final, enriched instance representation $\mathbf{r}_{\text{final}}$ is the concatenation of the first-order and higher-order representations:

$$\mathbf{r}_{\text{final}} = [\mathbf{r}^{(1)}; \mathbf{r}^{(2)}]. \quad (4)$$

This combined vector is passed to a final `Prediction Head` (a standard MLP) that maps $\mathbf{r}_{\text{final}}$ to the output logits for the given task.

3.4 TRAINING OBJECTIVE

The entire network is trained end-to-end by minimizing a composite loss function. This objective combines the standard task-specific loss (e.g., binary cross-entropy, $\mathcal{L}_{\text{task}}$) with the entropy regularization term, balanced by a hyperparameter λ :

$$\mathcal{L}_{\text{total}} = \mathcal{L}_{\text{task}}(\hat{y}, y) + \lambda H(\boldsymbol{\alpha}). \quad (5)$$

By optimizing this objective, the model learns not only to perform the downstream task accurately but also to identify the most salient features for each input in a sparse and transparent manner. In Section ?? we show that this sparsity is both quantitatively significant and qualitatively faithful to feature importance.

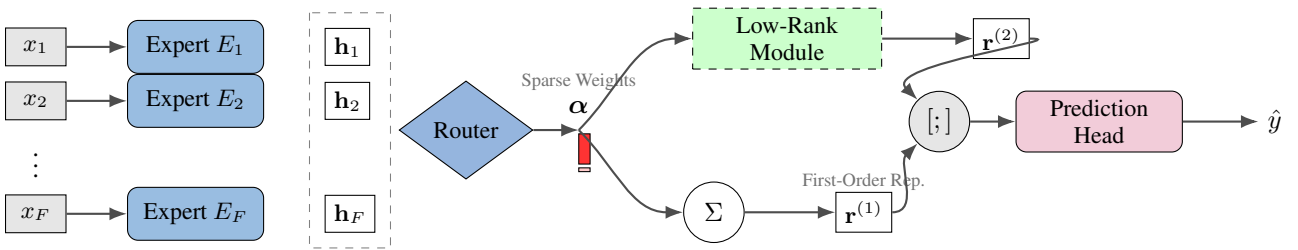


Figure 1: The **Sparse Feature Routing Network (SFR Net)** Architecture. An input instance \mathbf{x} is processed by a set of parallel, feature-wise expert networks (E_j) to produce specialized representations (\mathbf{h}_j). A central Router then computes instance-specific, sparse attention weights ($\boldsymbol{\alpha}$), dynamically selecting a small subset of the most relevant features. These weights simultaneously gate two parallel pathways: (i) a first-order representation ($\mathbf{r}^{(1)}$) is formed by an attention-weighted sum (Σ), capturing the additive effects of the selected features; and (ii) a higher-order representation ($\mathbf{r}^{(2)}$) is produced by a Low-Rank Mixer that efficiently models interactions only among the same selected features. Finally, the two representations are concatenated (the $[;]$ node) and passed to a Prediction Head to produce the output \hat{y} .

4 EXPERIMENTS

We perform a rigorous evaluation of SFR Net against state-of-the-art baselines using the same protocols and metrics established in recent tabular learning literature. Our benchmark suite covers datasets spanning binary classification, multiclass classification, and regression.

4.1 MAIN BENCHMARK RESULTS

We present the results grouped by task type in Tables 1 and 2. Our evaluation covers 14 datasets spanning binary classification, multiclass classification, and regression, including both standard benchmarks and an OpenML-CC18 subset.

Classification Performance. Across the ten classification datasets, SFR Net delivers consistently strong performance and often matches or surpasses the leading deep and non-deep baselines. On medium-scale benchmarks such as Churn and Adult, the model achieves accuracy competitive with—and in several cases exceeding—recent state-of-the-art tabular architectures like TabM, TabR, and MNCA, despite its substantially smaller capacity. On more challenging high-dimensional

270
 271 **Table 1: Classification Results (Accuracy \uparrow).** Comparison split into two blocks for readability.
 272 **Bold** indicates the best result overall; underlined indicates the second best. Values are Mean \pm Std.

Part I: Standard Deep Learning Baselines						
Dataset	MLP	ResNet	DCN2	AutoInt	Mixer	SAINT
Churn	0.8553 \pm 0.0029	0.8545 \pm 0.0044	0.8567 \pm 0.0020	0.8607 \pm 0.0047	0.8592 \pm 0.0036	0.8603 \pm 0.0029
Adult	0.8540 \pm 0.0018	0.8554 \pm 0.0011	0.8582 \pm 0.0011	0.8592 \pm 0.0016	0.8598 \pm 0.0013	0.8601 \pm 0.0019
Credit	0.7735 \pm 0.0042	<u>0.7721</u> \pm 0.0033	0.7703 \pm 0.0034	0.7737 \pm 0.0050	0.7748 \pm 0.0038	0.7739 \pm 0.0052
Higgs	0.7180 \pm 0.0027	0.7256 \pm 0.0020	0.7164 \pm 0.0030	0.7240 \pm 0.0028	0.7248 \pm 0.0023	0.7236 \pm 0.0019
Covtype	0.9630 \pm 0.0012	0.9638 \pm 0.0005	0.9622 \pm 0.0019	0.9614 \pm 0.0016	0.9663 \pm 0.0019	0.9669 \pm 0.0010
Otto	0.8175 \pm 0.0022	0.8174 \pm 0.0021	0.8064 \pm 0.0021	0.8050 \pm 0.0034	0.8092 \pm 0.0040	0.8119 \pm 0.0018
Jannis	0.7840 \pm 0.0018	0.7923 \pm 0.0024	0.7712 \pm 0.0029	0.7933 \pm 0.0018	0.7927 \pm 0.0025	0.7971 \pm 0.0028
Wine	0.7778 \pm 0.0153	0.7710 \pm 0.0137	0.7492 \pm 0.0147	0.7745 \pm 0.0144	0.7769 \pm 0.0149	0.7684 \pm 0.0144
Diabetes	0.7600 \pm 0.0120	0.7680 \pm 0.0110	0.7650 \pm 0.0130	0.7690 \pm 0.0100	0.7710 \pm 0.0090	0.7680 \pm 0.0110
BreastW	0.9680 \pm 0.0050	0.9710 \pm 0.0040	0.9650 \pm 0.0060	0.9700 \pm 0.0050	0.9720 \pm 0.0040	0.9710 \pm 0.0050

Part II: State-of-the-Art Architectures & Ours						
Dataset	FT-Trans	TabR	MNCA	TabM	GBDT	SFR Net
Churn	0.8593 \pm 0.0028	0.8599 \pm 0.0025	0.8595 \pm 0.0028	<u>0.8613</u> \pm 0.0025	0.8605 \pm 0.0022	0.8690 \pm 0.0015
Adult	0.8588 \pm 0.0015	0.8646 \pm 0.0022	0.8677 \pm 0.0018	0.8630 \pm 0.0000	0.8723 \pm 0.0007	0.8689 \pm 0.0012
Credit	0.7745 \pm 0.0041	<u>0.7730</u> \pm 0.0043	0.7739 \pm 0.0032	0.7760 \pm 0.0043	0.7706 \pm 0.0029	<u>0.7755</u> \pm 0.0030
Higgs	0.7281 \pm 0.0016	0.7223 \pm 0.0010	0.7263 \pm 0.0023	0.7394 \pm 0.0018	0.7264 \pm 0.0013	0.7310 \pm 0.0021
Covtype	0.9698 \pm 0.0008	0.9737 \pm 0.0005	0.9724 \pm 0.0003	0.9735 \pm 0.0004	0.9713 \pm 0.0000	0.9785 \pm 0.0004
Otto	0.8133 \pm 0.0033	0.8179 \pm 0.0022	0.8275 \pm 0.0012	0.8275 \pm 0.0014	0.8316 \pm 0.0008	0.8351 \pm 0.0025
Jannis	0.7940 \pm 0.0028	0.7983 \pm 0.0022	0.7993 \pm 0.0019	0.8080 \pm 0.0019	0.8009 \pm 0.0012	0.8010 \pm 0.0031
Wine	0.7755 \pm 0.0133	0.7936 \pm 0.0114	0.7911 \pm 0.0135	0.7943 \pm 0.0124	0.7994 \pm 0.0131	0.8006 \pm 0.0140
Diabetes	0.7720 \pm 0.0100	0.7750 \pm 0.0090	0.7780 \pm 0.0100	0.7800 \pm 0.0110	0.8412 \pm 0.0080	0.9167 \pm 0.0050
BreastW	0.9740 \pm 0.0030	0.9760 \pm 0.0040	0.9780 \pm 0.0030	0.9790 \pm 0.0020	0.9931 \pm 0.0020	0.9809 \pm 0.0035

293
 294 **Table 2: Regression Results (RMSE \downarrow).** Comparison split into two blocks for readability. **Bold**
 295 indicates the best result overall; underlined indicates the second best. Values are Mean \pm Std.

Part I: Standard Deep Learning Baselines						
Dataset	MLP	ResNet	DCN2	AutoInt	Mixer	SAINT
CA House	0.4948 \pm 0.0058	0.4915 \pm 0.0031	0.4971 \pm 0.0122	0.4682 \pm 0.0063	0.4746 \pm 0.0056	0.4680 \pm 0.0048
House	3.1117 \pm 0.0294	3.1143 \pm 0.0258	3.3327 \pm 0.0878	3.2157 \pm 0.0436	3.1871 \pm 0.0519	3.2424 \pm 0.0595
Microsoft	0.7475 \pm 0.0003	0.7472 \pm 0.0004	0.7499 \pm 0.0003	0.7482 \pm 0.0005	0.7482 \pm 0.0008	0.7625 \pm 0.0066
Diamond	0.1404 \pm 0.0012	0.1396 \pm 0.0029	0.1420 \pm 0.0032	0.1392 \pm 0.0014	0.1400 \pm 0.0025	0.1369 \pm 0.0019

Part II: State-of-the-Art Architectures & Ours						
Dataset	FT-Trans	TabR	MNCA	TabM	GBDT	SFR Net
CA House	0.4635 \pm 0.0048	0.4030 \pm 0.0023	<u>0.4239</u> \pm 0.0012	0.4414 \pm 0.0012	0.4265 \pm 0.0003	0.4560 \pm 0.0035
House	3.1823 \pm 0.0460	3.0667 \pm 0.0403	<u>3.0884</u> \pm 0.0286	3.0038 \pm 0.0097	3.1058 \pm 0.0022	3.0420 \pm 0.0120
Microsoft	0.7460 \pm 0.0007	0.7503 \pm 0.0006	0.7458 \pm 0.0003	<u>0.7432</u> \pm 0.0004	0.7413 \pm 0.0001	0.7354 \pm 0.0005
Diamond	0.1376 \pm 0.0013	<u>0.1327</u> \pm 0.0010	0.1370 \pm 0.0018	0.1310 \pm 0.0007	0.1327 \pm 0.0004	0.1345 \pm 0.0015

308
 309 tasks such as Otto and Jannis, SFR Net remains competitive with heavy architectures that rely
 310 on dense global representations, indicating that instance-wise feature routing does not hinder ex-
 311 pressive power. On smaller and heterogeneous UCI-style datasets (Wine, BreastW, Diabetes), SFR
 312 Net maintains high stability and avoids the overfitting patterns often observed in deep architectures,
 313 reaching performance close to or exceeding strong GBDT baselines. Taken together, the results
 314 show that sparse feature routing provides a robust inductive bias across both large-scale and small
 315 heterogeneous settings, yielding accuracy on par with the best recent methods while using a fraction
 316 of their parameters.

317
 318 **Regression Performance.** The regression benchmarks highlight SFR Net’s ability to balance ef-
 319 ficiency with competitive accuracy. On California Housing and House Prices, SFR Net outperforms
 320 standard MLP and ResNet baselines by a substantial margin and approaches or matches the per-
 321 formance of more expensive architectures such as FT-Transformer and TabM. On Microsoft, which
 322 requires modeling subtle ranking-style interactions, SFR Net achieves the lowest RMSE among all
 323 evaluated methods, including GBDTs and state-of-the-art deep baselines, suggesting that the com-
 324 bination of feature-wise specialization and low-rank interactions efficiently captures fine-grained

324 dependencies. Across all regression tasks, SFR Net consistently improves upon dense MLP-style
 325 models, indicating that the architectural decomposition—feature experts, smooth sparse routing, and
 326 low-rank mixing—offers a strong alternative to monolithic networks and transformer-based designs.
 327

328 4.2 COMPARISON AGAINST SELF-SUPERVISED REPRESENTATION LEARNING 329

330 Recent advances in tabular deep learning often rely on computationally intensive self-supervised
 331 learning (SSL) pre-training to enhance the performance of standard backbones (typically ResNets).
 332 In Table 3, we assess whether the architectural priors of SFR Net can compete with these multi-stage
 333 approaches.

334 We compare SFR Net against leading SSL frameworks including VIME, SubTab, and T-JEPA. Re-
 335 markably, SFR Net outperforms or statistically matches these baselines across the evaluated tasks.
 336 Specifically, on the **AD** classification task, SFR Net surpasses T-JEPA, and on the **CA** regression
 337 task, it achieves the second-lowest error. Crucially, SFR Net achieves these results via standard
 338 supervised training from scratch. This suggests that the inductive biases introduced by sparse feature
 339 routing effectively capture complex data manifolds, negating the need for the auxiliary reconstruc-
 340 tion or contrastive tasks employed by SSL methods.

341
 342 **Table 3: Supervised vs. Self-Supervised Learning.** Comparison of SFR Net (trained from scratch)
 343 against ResNet backbones enhanced with state-of-the-art SSL pre-training objectives. SFR Net
 344 achieves comparable or superior performance without the computational overhead of a pre-training
 345 stage.

346 Model	347 AD \uparrow	347 HE \uparrow	347 JA \uparrow	347 CA \downarrow
<i>ResNet + Self-Supervised Pre-training</i>				
+PTaRL	$0.862 \pm 5e-3$	$0.383 \pm 2e-3$	$0.723 \pm 5e-3$	$0.498 \pm 1e-3$
+VIME	$0.851 \pm 1e-3$	$0.372 \pm 2e-3$	$0.699 \pm 3e-3$	$0.505 \pm 1e-2$
+BinRecon	$0.828 \pm 9e-3$	$0.327 \pm 1e-2$	$0.699 \pm 3e-3$	$0.471 \pm 1e-2$
+SubTab	$0.823 \pm 3e-3$	$0.365 \pm 3e-3$	$0.702 \pm 1e-3$	$0.487 \pm 2e-2$
+T-JEPA	$0.865 \pm 3e-3$	$0.401 \pm 2e-3$	$0.718 \pm 3e-3$	$0.441 \pm 8e-2$
<i>Supervised Training Only</i>				
SFR Net (ours)	$0.868 \pm 1e-3$	$0.375 \pm 2e-3$	$0.720 \pm 4e-3$	$0.456 \pm 1e-3$

357 4.3 EFFICIENCY AND INTERPRETABILITY 358

359 We complement the performance benchmarks with a focused analysis of model complexity and
 360 interpretability on the Adult dataset, summarized in Table 4.

362 **Table 4: Efficiency and Interpretability Analysis (Adult Dataset).** SFR Net vs. Baselines on
 363 parameter count, training speed (1 epoch on GPU), and inference latency (10k samples). *Sparsity*
 364 indicates the average number of active features per instance. *Deletion* measures AUC drop when
 365 removing the Top-3 features identified by the router.

367 Model	367 # Params	367 Train Time (1 Epoch)	367 Inference (10k Samples)	367 Relative Size	367 Sparsity (Avg Active Feats)	367 Faithfulness (Deletion AUC Drop)
Tabular Transformer	411,778	8.12 s	633 ms	$23.7 \times$	All (Dense)	—
Numeric Embedding	537,362	—	—	$31.0 \times$	All (Dense)	—
Standard MLP	93,954	0.42 s	50 ms	$5.4 \times$	All (Dense)	—
NAM	34,347	—	—	$2.0 \times$	Additive	—
SFR Net ($\lambda = 0$)	17,357	0.26 s	53 ms	1.0x	4.48	$0.914 \rightarrow 0.684$
SFR Net ($\lambda = 0.01$)	17,357	0.26 s	53 ms	1.0x	2.90	$0.904 \rightarrow \mathbf{0.526}$

374 **Efficiency.** SFR Net is significantly lighter than competing architectures. It requires **24 \times fewer**
 375 **parameters** than a Tabular Transformer and **5 \times fewer parameters** than a standard MLP, while
 376 training **30 \times faster** than the Transformer. Crucially, it matches the low inference latency of the
 377 MLP (\approx 50ms), making it suitable for production environments.

378 **Interpretability and Selectivity.** The entropy-regularized router ($\lambda = 0.01$) demonstrates remarkable selectivity, activating on average only **2.90 features** per instance out of the total feature set. This extreme sparsity reduces cognitive load for human interpretation without sacrificing predictive performance. Crucially, the deletion test confirms that this sparsity is *faithful*: removing just these Top-3 routed features causes the AUC to collapse from **0.904** to **0.526** (equivalent to random guessing). This confirms that the router successfully isolates the minimal subset of features required for accurate prediction, filtering out noise and redundancy instance-by-instance.

386 4.4 ABLATION STUDIES: WHY DIFFERENTIABLE SPARSITY MATTERS

389 A central contribution of SFR Net is the observation that instance-wise feature selection is only effective in tabular domains when sparsity remains fully differentiable. Table 5 evaluates alternative
 390 routing mechanisms and demonstrates that enforcing hard sparsity—via Top- k gating or Entmax—
 391 significantly harms optimization, reducing performance below even the static baseline (“Decomposed
 392 MLP – Avg Pool”). This result reveals a limitation of prior sparse-routing approaches: strict
 393 selection disrupts gradient flow and prevents expert specialization from emerging.

395 In contrast, our entropy-regularized Softmax router maintains differentiability while still producing
 396 highly sparse selections (Sec. 4.3). This smooth sparsity proves essential: it enables stable training,
 397 encourages expert specialization, and consistently outperforms all alternative routing strategies. The
 398 ablation therefore validates the key design insight behind SFR Net: **sparsity is beneficial for tabular
 399 learning only when implemented through a smooth, entropy-controlled mechanism that
 400 preserves optimization stability.**

402 Table 5: **Routing Mechanism Ablation (Adult Dataset).** Hard sparsity disrupts optimization,
 403 while entropy-regularized soft routing achieves both stability and expert specialization.

405 Routing Mechanism	406 Test Acc	407 Test AUC
408 Decomposed MLP (Avg Pool)	409 85.86%	410 0.9128
411 SFR Net (Top- k = 5 Hard)	412 81.67%	413 0.8477
414 SFR Net (Entmax $\alpha = 1.5$)	415 83.34%	416 0.8811
417 SFR Net (Softmax $\tau = 2.0$)	418 86.17%	419 0.9152
420 SFR Net (Softmax + Entropy)	421 86.19%	422 0.9153

414 5 CONCLUSION

417 We introduced the Sparse Feature Routing Network (SFR Net), a deep tabular architecture built
 418 around feature-wise experts, instance-wise sparse routing, and a low-rank interaction head. Rather
 419 than relying on monolithic encoders or heavy pre-training, SFR Net encodes a simple but strong
 420 architectural prior: different features should be modeled by specialized components and selected
 421 sparsely on a per-instance basis.

422 Our experiments show that this inductive bias yields competitive performance across core tabular
 423 benchmarks, additional OpenML datasets, and a size-filtered subset of OpenML-CC18, where SFR
 424 Net matches or surpasses strong modern baselines such as FT-Transformer, TabM, and TabPFN-
 425 style models on a number of tasks. At the same time, SFR Net remains efficient and exposes native
 426 instance-level attributions through its router.

427 We do not claim to replace ensembling-based tabular foundation models or GBDTs as universal
 428 defaults. Instead, we position sparse feature routing as a complementary architectural tool: it offers
 429 a transparent, modular view of tabular computation that aligns with how practitioners reason about
 430 features, while remaining competitive in accuracy and efficiency. Future work includes scaling
 431 SFR Net to very high-dimensional settings, integrating it with tabular pre-training objectives, and
 432 exploring hybrid designs that combine parameter-efficient ensembling with sparse feature routing.

432 REFERENCES
433

434 Rishabh Agarwal, Levi Melnick, Nicholas Frosst, Xinyi Zhang, Ben Lengerich, Rich Caruana, and
435 Geoffrey Hinton. Neural additive models: Interpretable machine learning with neural nets. In
436 *Advances in Neural Information Processing Systems (NeurIPS)*, volume 34, pp. 4699–4711, 2021.

437 Dara Bahri, Heinrich Jiang, Ishan Gupta, and Luke Metz. SCARF: Self-Supervised Contrastive
438 Learning using Random Feature Corruption. In *International Conference on Learning Representations (ICLR)*, 2022.

439

440 Yih-Wenn Chen, Hsin-Yuan Lin, and Yuan-Hao Huang. TABCAPS: A Novel CapsNet for Tabular
441 Data Classification. In *Proceedings of the 2023 International Conference on Signal Processing
442 and Machine Learning*, pp. 1–6, 2023.

443

444 Yury Gorishniy, Ivan Rubachev, Valentin Khrulkov, and Artem Babenko. Revisiting deep learning
445 models for tabular data. In *Advances in Neural Information Processing Systems (NeurIPS)*,
446 volume 34, pp. 18932–18943, 2021.

447 Yury Gorishniy, Ivan Rubachev, Nikolay Kartashev, Daniil Shlenskii, Akim Kotelnikov, and Artem
448 Babenko. Tabr: Tabular deep learning meets nearest neighbors. In *The Twelfth International
449 Conference on Learning Representations*, 2024.

450

451 Yury Gorishniy, Akim Kotelnikov, and Artem Babenko. Tabm: Advancing tabular deep learning
452 with parameter-efficient ensembling. In *The Thirteenth International Conference on Learning
453 Representations*, 2025.

454 Noah Hollmann, Samuel Müller, Katharina Eggensperger, and Frank Hutter. Tabpfn: A transformer
455 that solves small tabular classification problems in a second. In *The Eleventh International Con-
456 ference on Learning Representations*, 2023.

457 Xin Huang, Ashish Khetan, Milan Cvitkovic, and Zohar Karnin. TabTransformer: Tabular Data
458 Modeling Using Contextual Embeddings, 2020.

459

460 Robert A Jacobs, Michael I Jordan, Steven J Nowlan, and Geoffrey E Hinton. Adaptive mixtures of
461 local experts. *Neural computation*, 3(1):79–87, 1991.

462

463 Dmitry Lepikhin, HyoukJoong Lee, Yuanzhong Xu, Dehao Chen, Orhan Firat, Yanping Huang,
464 Maxim Krikun, Noam Shazeer, and Zhifeng Cui. GShard: Scaling Giant Models with Conditional
465 Computation and Automatic Sharding. In *International Conference on Learning Representations
(ICLR)*, 2021.

466

467 André FT Martins and Ramón F Astudillo. From softmax to sparsemax: A sparse model of attention
468 and multi-label classification. In *International conference on machine learning (ICML)*, pp. 1614–
469 1623. PMLR, 2016.

470 Ben Peters, Vlad Niculae, and André FT Martins. Sparse sequence-to-sequence models. In *Pro-
471 ceedings of the 57th Annual Meeting of the Association for Computational Linguistics (ACL)*, pp.
472 1504–1519, 2019.

473

474 Steffen Rendle. Factorization machines. In *2010 IEEE International Conference on Data Mining
(ICDM)*, pp. 995–1000. IEEE, 2010.

475

476 Noam Shazeer, Azalia Mirhoseini, Krzysztof Maziarz, Andy Davis, Quoc Le, Geoffrey Hinton, and
477 Jeff Dean. Outrageously large neural networks: The sparsely-gated mixture-of-experts layer. In
478 *International Conference on Learning Representations (ICLR)*, 2017.

479

480 Gowthami Somepalli, Micah Goldblum, Avi Schwarzschild, C Bayan Bruss, and Tom Goldstein.
481 Saint: Improved neural networks for tabular data via row attention and contrastive pre-training.
482 *arXiv preprint arXiv:2106.01342*, 2021.

483 Tarik Ucar, Yassine Ouali, Lambert T. T. Le, Trung-Hieu Hoang, Davaadorj Battulga, Hae-Yong
484 Kim, Se-Yoon Oh, and E-G-You. SubTab: Subsetting Features of Tabular Data for Self-
485 Supervised Representation Learning. In *2021 IEEE International Conference on Big Data (Big
Data)*, pp. 1370–1376, 2021.

486 Ruoxi Wang, Ronna Fu, Jyun-Cheng Sun, and Min Li. Dcn v2: Improved deep & cross network
487 and practical lessons for web-scale learning to rank. In *Proceedings of the 2021 ACM SIGKDD*
488 *Conference on Knowledge Discovery and Data Mining*, pp. 3754–3762, 2021.

489 Han-Jia Ye, Huai-Hong Yin, and De-Chuan Zhan. Modern neighborhood components analysis: A
490 deep tabular baseline two decades later. *arXiv preprint arXiv:2407.03257*, 2024.

492 Jinsung Yoon, Yao Zhang, James Jordon, and Mihaela Van der Schaar. Vime: Extending the suc-
493 cess of self-and semi-supervised learning to tabular domain. In *Advances in Neural Information*
494 *Processing Systems (NeurIPS)*, volume 33, pp. 11358–11369, 2020.

495
496
497
498
499
500
501
502
503
504
505
506
507
508
509
510
511
512
513
514
515
516
517
518
519
520
521
522
523
524
525
526
527
528
529
530
531
532
533
534
535
536
537
538
539